NUCL SCI TECH (2021) 32:43
https://doi.org/10.1007/s41365-021-00879-x

Investigation of ex-vessel core catcher for SBO accident in VVER-1000/V528 containment using MELCOR code

Farhad Salari[1] · Ataollah Rabiee[1] · Farshad Faghihi[1,2,3]

Received: 17 October 2020 / Revised: 5 January 2021 / Accepted: 27 January 2021 / Published online: 21 April 2021

Abstract To mitigate consequences of core melting, an ex-vessel core catcher is investigated in this study. Instructions should be obeyed to cool down the corium caused by core melting. The corium destroys the reactor containment and causes radioactive materials to be released into the environment if it does not cool down well. It is important to build a core catcher system for the reception, localization, and cool down of the molten corium during a severe accident resulting from core melting. In this study, the role of a core catcher in the VVER-1000/v528 reactor containment during a station black out (SBO) accident is evaluated using the MELCOR1.8.6 code. In addition, parametric analyses of the SBO for (i) SBO accidents with emergency core cooling system (ECCS) operation, and (ii) without ECCS operation are performed. Furthermore, thermal–hydraulic analyses in dry and wet cavities with/without water are conducted. The investigations include the reduction of gases resulting from molten–corium–concrete interactions (H_2, CO, CO_2). Core melting, gas production, and the pressure/temperature in the reactor containment are assessed. Additionally, a full investigation pertaining to gas release (H_2, CO, CO_2) and the pressure/temperature of the core catcher is performed. Based on MELCOR simulations, a core cavity and a perimeter water channel are the best options for corium cooling and a lower radionuclide release. This simulation is also theoretically investigated and discussed herein. The simulation results show that the core catcher system in addition to an internal sacrificial material reduces the containment pressure from 689 to 580 kPa and the corresponding temperature from 394 to 380 K. Furthermore, it is observed that the amount of gases produced, particularly hydrogen, decreased from 1698 to 1235 kg. Moreover, the presence of supporting systems, including an ECCS with a core catcher, prolonged the core melting time from 16,430 to 28,630 s (in an SBO accident) and significantly decreased the gases produced.

Keywords Core catcher · VVER-1000/V528 · Containment · SBO accident · MELCOR · Environmental radionuclide release · Corium cooling

Abbreviations

MCCI	Molten corium concrete interaction
BNPP	Bushehr nuclear power plant
ECCS	Emergency core cooling system
IVR	In-vessel melt retention
EVR	Ex-vessel melt retention
SM	Sacrificial material
LOOP	Loss of offside power
RPV	Reactor pressure vessel
SBO	Station black out
ACC	Accumulator
CC	Core catcher
PSD	Pulse safety device
SG	Steam generator
RCP	Reactor coolant pump

✉ Farshad Faghihi
faghihif@shirazu.ac.ir

[1] Department of Nuclear Engineering, School of Mechanical Engineering, Shiraz University, Shiraz 71936-16548, Iran

[2] Radiation Research Center, Shiraz University, Shiraz, Iran

[3] Ionizing and Non-Ionizing Research Center, Shiraz University of Medical Science, Shiraz, Iran

1 Introduction

Understanding the responses of the containment pressure and fission gases released during a severe accident is crucial to ensure public safety, as well as to allow operators to perform necessary actions to maintain containment integrity and mitigate the consequences of the accident [1]. In severe accidents resulting in core melting (corium), a core catcher is necessitated. Providing short- and long-term heat removal conditions from molten corium materials is one of the most important issues that should be considered after any core melting. Hence, various technical calculations to achieve stable controlled conditions must be investigated. If a molten corium does not cool down well, reactor containment will fail, thereby resulting in the release of hazardous radioactive materials to the public.

A core catcher (CC) performs the following main functions [2].

- Receives and retains the volume liquid and solid corium components, core, and reactor structural material debris;
- Provide stable heat transfer from corium to cooling water and reliable corium cool down; Ensures corium subcriticality in the concrete cavity during its cool down;
- Ensures the minimum release of radioactive materials and hydrogen into the containment space;
- Sustains the position of the reactor pressure vessel bottom head containing core debris during its deformation and rupture until corium is ejected into the concrete cavity;
- Protects elements of the concrete cavity and prevents them from thermo–mechanical effects of the pouring corium.

If the corium produced is below a definite amount and the cooling activity does not occur as intended, then a reaction will occur between the corium and the inner wall of the concrete. This phenomenon is known as a molten corium concrete interaction (MCCI), which releases various gases. Additionally, it increases the containment pressure of the reactor, thereby resulting in a greater dispersal of radioactive materials. Specifically, during an MCCI, hydrogen, CO, and CO_2 gases are produced.

To date, many studies pertaining to corium cooling have been conducted. The related activities performed can be classified into two categories: (i) corium cooling inside and (ii) outside of a vessel.

The internal cooling strategy is known as in-vessel melt retention (IVR). In this strategy, the outside vessel is immersed in water to reduce the corium temperature. This method prevents damage to the bottom of the reactor pressure vessel (RPV) structure. IVR was first introduced by Theofanous in 1989 at the University of California [3]. Since 1989, many studies have been performed based on IVR to design power plants with medium-power reactors, such as VVER-440 (Lovisa Finland) [4], AP600 (Westinghouse, USA) [5], and VVER-640 (SPBAEP, Russia) [6].

The outside cooling strategy is known as ex-vessel melt retention (EVR). To date, it has been investigated extensively using different reactors. In 1980, Löwenhielm et al. investigated molten cooling from outside an RPV in Swedish BWR, in which molten corium was analyzed based on a melting drop inside a pool of pool water [7]. The main issue in ex-vessel cooling is the occurrence of steam explosion.

The cooling strategy for reactor vessels using a CC system has been investigated for both western PWRs and VVERs, which are briefly described herein. For instance, Stevlov et al. evaluated a CC system for a VVER-1000 reactor at China's Tyanvan power plant [2]. In those studies, the conceptual design and justification of the CC were analyzed.

In 2006, a project to build a VVER-1200 reactor was implemented in Russia [8]. In this project, the design of the crucible-type CC system was considered. In 2011, Zvonarev et al. performed numerical calculations of a CC system using the GEFEST-URL computational code, and they analyzed the thermal behavior of molten corium [8]. The results obtained were as follows:

- Calculations showed that the molten corium could not escape from the wall of the CC vessel to the outside;
- the maximum temperature of the inner surface of the wall for several severe accident scenarios was lower than 1076 °C;
- the minimum margin for the mass flow rate on the outer surface of the CC system was approximately 3 kg/s;
- the maximum water vapor production rate was 14 kg/s when water was spilled on top of the molten surface; however, one hour later, the vapor flow decreased gradually and did not exceed 6 kg/s;
- the maximum amount of hydrogen produced in the CC system, as obtained from three hypothetical severe accidents, did not exceed 3 kg.

In 2009, Khabensky et al. investigated the justification of VVER-1000 reactors [9]. In that study, the role of the sacrificial material in corium cooling was confirmed. In 2010, Astafyeva et al. analyzed the molten behavior of a CC system for the LNPP-2006 reactor [10]. In that study, the CC system was modeled using the HEFEST code, which was developed in Russia.

In 2005, Sulatsky et al. conducted a laboratory study pertaining to the reaction of molten corium with oxidized

materials in a CC system of VVER reactors [11]. In that study, which was simulated using the CORCAT code, the code was validated with laboratory results, and the melt reaction with the sacrificial material was evident. Various studies have been conducted regarding the selection of sacrificial materials for the CC system, of which a summary is provided in [12].

In the current study, the role of a CC for the containment of VVER-1000/v528 during a station black out (SBO) accident was evaluated using the MELCOR1.8.6 code. In addition, parametric analyses of the SBO for (i) SBO accidents with emergency core cooling system (ECCS) operation and activation of accumulators, and (ii) without ECCS operation and inactivity of accumulators were performed. Herein, the material and methods are first highlighted. Subsequently, the SBO accident and plant safety features are described. MELCOR benchmarking was performed for SBO, LB-LOCA, and steady-state conditions. In addition, the obtained results, including those of H_2 and other gases released, are discussed. Finally, a theoretical investigation was performed for the best "CC + cavity" obtained, which is described in detail herein.

2 Material and methods

In the current section, the problem is defined. Additionally, information regarding a case study and its safety features, as well as MELCOR descriptions and nodalizations are provided.

2.1 Sacrificial material

A reactor safety system is designed to prevent various phenomena, including the direct heating of the reactor containment due to the injection of high-pressure molten corium into the cavity, vapor explosion, and MCCIs. The molten corium material enters the CC system and combines with the sacrificial material to reduce the molten temperature. Within the CC system, the six roles of the sacrificial material are as follows [2]:

- Decreases the melt corium temperature by the endothermic effect during the corium–sacrificial material reaction;
- increases the molten volume and provides a greater heat transfer level between the corium and cooling water; reduces the thermal flux in the walls and increases the safety margin of the critical thermal flux;
- decreases the corium chemical activity due to the oxidation of its elements by the oxides of the sacrificial material;
- minimizes hydrogen production during the oxidation of zirconium in the corium to prevent hydrogen explosion;
- ensures the subcriticality of the molten corium;
- inverses the oxide and steel layers in the corium pool.

It is noteworthy that a few CC designs for VVER- and EPR-type reactors have been realized based on two different approaches. Figure 1 shows the CC designs for both reactor types.

In the VVER design, the CC is crucible-type system that contains the sacrificial material and is located under the RPV. In this case, the corium combines with the sacrificial material, and its temperature decreases owing to the above-mentioned six roles of the sacrificial material. In addition, the water flow around the CC can be considered as an additional decay heat removal system.

The first practical design of these systems was developed by the Russians for VVER-1000-type reactors at the Tyanvan China Power Plant and the Indian Kudankulam Power Plant [9], where the CC of the Tyanvan China reactor was initially built.

Another case is a CC for the EPR, which comprises a core melt stabilization system located on the lateral side of the RPV. The stabilization system is intended to first spread the melt and then execute cooling operations. The EPR CC was held under the reactor vessel designed by Fischer et al. [13]. Figure 1b shows a schematic view of the EPR CC. In this case, the corium was transferred into a flat and wide area to reduce its temperature and avoid its neutronics criticality.

2.2 Current case study: VVER-V528

The current operational Bushehr nuclear power plant (BNPP) is of the VVER-1000-v446 type. The VVER-1000-V528 reactor is associated with the second phase of the BNPP and is currently under investigation and pre-construction for future operation. It is noteworthy that the first phase of the BNPP, which is currently operating, comprises a VVER-1000/v446 reactor without a core catcher system, and the second phase of this power plant, which is under development, will comprise a VVER-1000/v528 reactor including a CC system. Based on the similarity between both VVERs (except for minor cases in the core, such as fuel rod enrichment, dimensions, mixed Gd, and control rod patterns), the first and second circuits of the VVER-1000/V446 as well as the reactor containment were modeled.

2.2.1 Containment Information

The BNPP containment belongs to the category of lower-atmospheric containment. To satisfy construction

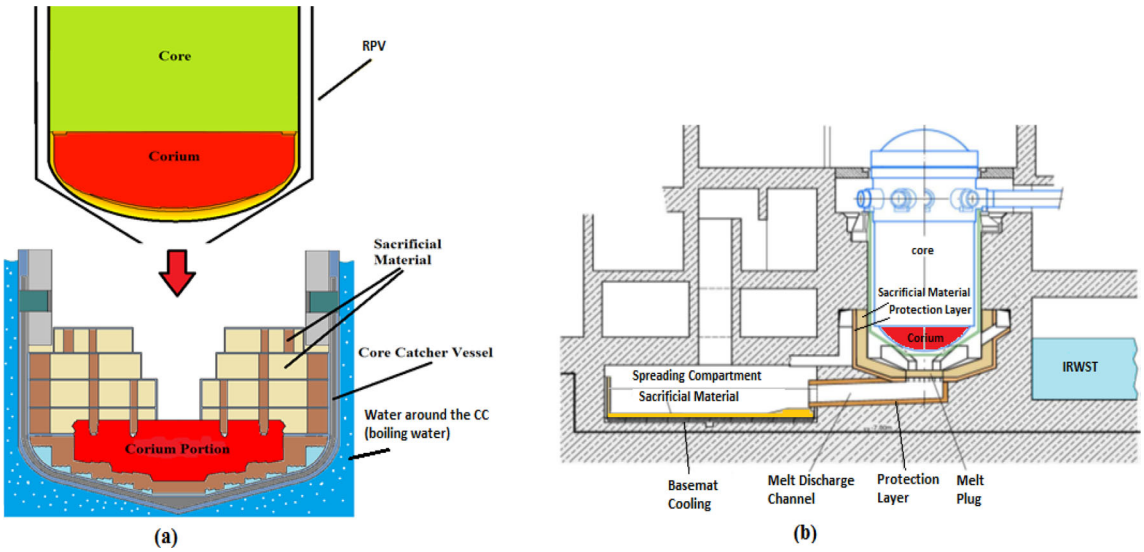

Fig. 1 (Color online) Schemes of CC for VVER and EPR reactors. **a** Cooling method of corium in VVER reactors. **b** Cooling method of corium in EPR reactors [13]

safety requirements, it was constructed based on dual-layer containment, an outer cast-in-situ reinforced concrete, and an inner spherical steel [14]. Some of the containment specifications are listed in Table 1.

2.2.2 *Dimensions of Primary-Loop Pipelines*

The primary circuit of the BNPP comprises one pressurizer and four coolant loops. Each loop comprises one steam generator, a main coolant pump, and 300 mm pipe lines. Figure 2 shows the layout of the primary circuit, which was applied in the current study. For more details regarding the steady-state data, one can refer to [16–18].

2.2.3 *Emergency Systems for SBO BDBA*

For managing severe accidents, such as the SBO accident, two basic emergency systems are available, as follows:

(i) High-pressure protection systems in primary and secondary loops. In the primary loop, safety valves in the pressurizer control the high-pressure signals. In the secondary loop, steam control valves are used to control high steam pressures. Table 2 lists their set points [19].

Table 1 BNPP containment specifications [15]

Parameters	Values
Structural parameters	
Steel containment inner diameter (mm)	28,000
Steel thickness (mm)	30
Gap thickness (mm)	1650
Concrete thickness (mm)	1750
Containment free volume (m^3)	71,040
Design parameters	
Maximum internal pressure at 150 °C (MPa)	0.46
Maximum pneumatic test pressure at a temperature of up to 60 C (MPa)	0.51
Peak temperature (in a separate compartment) (°C)	Up to 206 °C during 5 min
Maximum (averaged over the volume) temperature (°C)	150
Main heat sinks inside containment	
Total area of all concrete walls (m^2)	18,860
Surface area of steel containment, effective area of metal structures, and equipment without heat insulation (m^2)	17,712

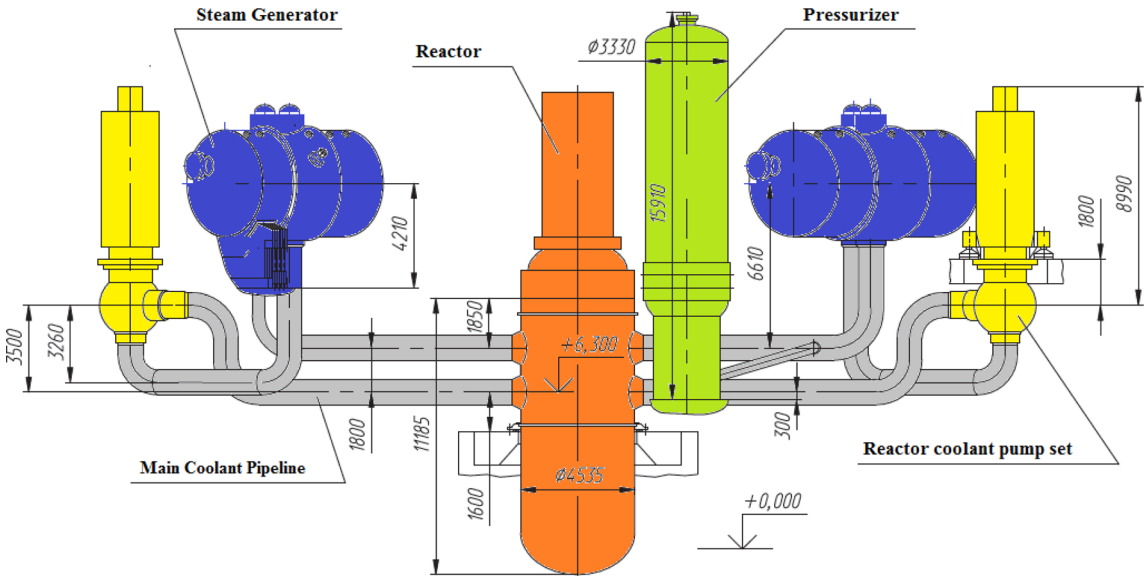

Fig. 2 (Color online) Primary circuit pipelines of BNPP

Table 2 Settings of high-pressure protection systems in primary and secondary loops [19]

Parameters	Value
PRIMARY SIDE: Safety and controlling valves in the pressurizer (PSD in primary loop)	
One control valve: Opening-Closing set points (MPa)	18.1–17.2
Two safety valves: Opening-Closing set points (MPa)	18.6–17.6
Elapsing time for Opening/Closing (s)	1.0–5.0
SECONDARY SIDE: Safety and controlling valves in the SGs (PSD in secondary loop)	
One valve called the control valve: Opening-Closing set points (MPa)	8.24–6.87
One valve called the safety valve: Opening-Closing set points (MPa)	8.44–6.87
Elapsing time for Opening-Closing (s)	1.0–1.0
(BRU-A) valves set-points Opening-Closing (in the SGs)(MPa)	7.15–6.27
Elapsing time for electrically Opening-Closing (s)	15.0–15.0

(ii) Boric acid insertion systems—high- and low-pressure Insertion systems. During accidents, ECCS accumulators are operated if the pressure is less than 5.88 MPa, whereas KWU tanks are operated if the pressure is less than 2.5 MPa. Table 3 lists the necessary parameters and set points [19].

The ECCS accumulators are directly connected to the reactor pressure chamber and reactor collection chamber, whereas the KWU tanks, high-pressure injection system, and low-pressure injection system are connected by pipelines to both hot and cold legs (with a nominal pipe diameter of 0.3 m).

2.2.3.1 Instruments in primary side for pressure control after LOOP and SBO A few instruments and/or practical instructions are applicable following LOOP or SBO accidents, as follows:

- The control valves will be automatically opened (DC power supplies) if the primary pressure is exceeds 18.1 MPa, and the safety valves will be opened if the primary pressure exceeds 18.6 MPa. Furthermore, the safety and control valves will be automatically closed at 17.6 and 17.2 MPa, respectively (c.f., Table 2);
- the valves can be opened manually by the operator for steam removal (during a LOOP accident)—a few minutes are required to open and close them (at least 5 min).

Opening the PRZ PSD and steam removal are necessary to reduce the primary pressure as well as the possible use of water inventory in the ECCS and KWU accumulators.

Table 3 Information pertaining to four ECCS accumulators and eight KWU tanks used in this study [19]

Parameters	Value
Number of ECCS accumulators	4
Total volume of ECCS accumulators (m^3)	60
Initial volume of nitrogen gas in ECCS accumulator (m^3)	10
Water content in each ECCS accumulator (m^3)	50
Nominal pressure in ECCS accumulator (MPa)	5.88
Water temperature in ECCS accumulator (°C)	60–70
Boric acid concentration in ECCS accumulator, gr-(H_3BO_3)/kg-(H_2O)	16
Number of KWU accumulators	8
Total volume of an accumulator (m^3)	45
Volume of boron acid in tank (m^3)	38
Volume of nitrogen gas in tank (m^3)	7
Operating pressure (MPa)	2.5
Operating temperature (°C)	60
Boric acid concentration, g-(H_3BO_3)/kg-(H_2O)	16

Primary side steam removal is one of the methods for core cooling during accidents such as LOOP and SBO.

2.2.3.2 Instruments in secondary side for pressure control after LOOP and SBO During an SBO, the BRU-A valves will be supplied by the DC power, and when all DC power are supplied, the BRU-A valves are maintained in their current status (open/closed). The following set points apply to the secondary side [19]:

- The BRU-A valves open (automatically) at 7.15 MPa;
- the BRU-A valves control the secondary-loop operating pressure to 6.67 MPa;
- if the secondary pressure is less than 6.27 MPa, then the BRU-A valves are closed;
- in cases involving SBO and loss of DC supply, the BRU-A valves maintain their current status;
- the BRU-A valves can be opened/closed when no DC power is available (5–10 min),

It must be emphasized that other types of safety valves exist (in the SGs) such during the loss of AC and/or DC power (when BRU-A valves do not function electrically), they function under secondary pressures and their spring stiffness. Those valves are opened if the pressure exceeds 8.24/8.44 MPa (c.f., Table 2), whereas they are closed when the pressure is less than 6.87 MPa.

2.3 MELCOR code

In our study, we used the MELCOR code to evaluate the CC system and perform a TH analysis.

MELCOR is a fully integrated, engineering-level computer code that models the progression of severe accidents in LWRs; it was developed by Sandia National Laboratories for the U.S. Nuclear Regulatory Commission [20]. The MELCOR code models a wide range of physical phenomena, including thermal hydraulics, heat transfer, aerosol physics, heat-up, degradation, relocation of reactor cores, ex-vessel debris behavior, fission product release, and H_2 production.

MELCOR is executed in two parts [20]: The first part is known as MELGEN, in which the majority of the input is specified, verified, and processed. When the input verification is satisfied, a restart file is written for the initial conditions. The second part is the MELCOR program, which solves the time-dependent problem using MELGEN and any other boundaries. Finally, post-processing graphics are provided by the HISPLT module.

It is noteworthy that because VER-type reactors are Russian-type reactors, most related studies thus far have been conducted by modeling severe power plant accidents using MELCOR. For instance, in recent studies [15, 21–24], the Bulgarian VVER-1000/v320 reactor can be cited as a MELCOR simulation [25–28].

2.3.1 Containment modeling

The containment building was partitioned into 23 cells, of which each included 33 engineering-VENTS, as shown in Fig. 3. As presented in Fig. 3, each cell can be connected to the other cells. For instance, cells 2 and 8, cells 2 and 9, cells 2 and 21, cells 3 and 10, cells 3 and 11, and cells 3 and 21 are defined as VALVE. The details of each cell are listed in Table 4. In this study, the containment structure and its instruments were modeled using 509 heat structures, which included walls, roofs, and floors, as described in Table 4.

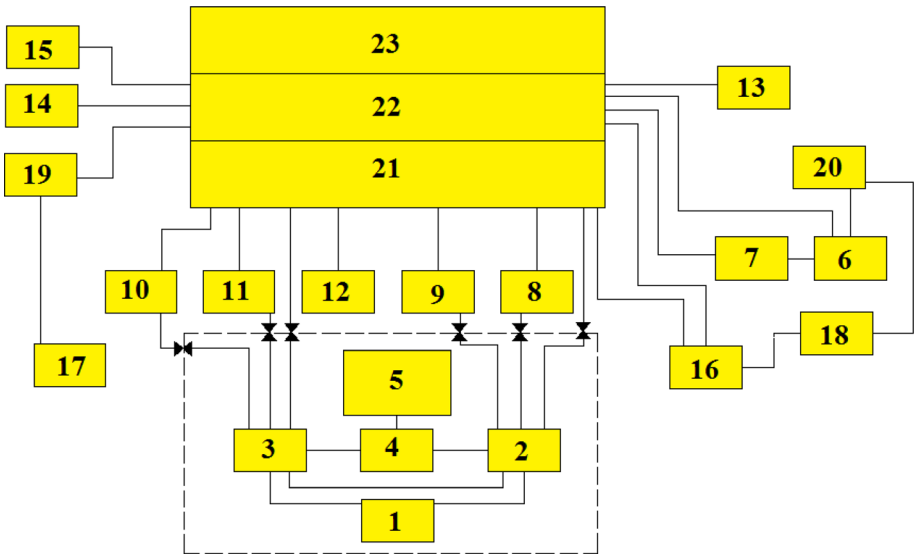

Fig. 3 (Color online) Definition of CELL, VENT, and VALVE in MELCOR

Table 4 BNPP containment cell specifications [29]

Cell number	Description of cell	Free volume (m^3)
1	Room for leakage collection	620
2	Rooms of SG compartment, pressurizer, and filters	4938
3	Rooms of SG compartment, bubbler, and filters	5050
4	Reactor vault	345
5	Reactor vault, reactor internal pool	925
6	Vaults of steam pipelines, feed water pipelines, and adjoining rooms	233
7	Vaults of steam pipelines, feed water pipelines, and adjoining rooms	265
8	RCP room	197
9	RCP room	214
10	RCP room	205
11	RCP room	205
12	Fuel cooling pool and cask storage pool	1467
13	Fresh fuel storage facility	600
14	Room of filtering installation and air recirculation	645
15	Room of filtering installation and air recirculation	645
16	TF system valve chambers	443
17	Staircases, adjoining rooms under fuel cooling pool, TU system valve chamber, and pumps of RCP oil cooling system. Chamber of process monitoring transducers. Oil cooler pump of fourth loop	1350
18	Staircases, adjoining rooms, chamber of backup converter. Pumps of RCP oil cooling system, pipelines	660
19	TA system valve chambers	930
20	Passage along containment perimeter	139
21	Room of TA system high-pressure cooler	21,100
22	Reactor hall space inside cylindrical wall	14,480
23	Reactor hall space between cylindrical wall and steel containment	16,000
	Reactor hall space above cylindrical wall	

2.3.2 *Modeling of primary–secondary circuits, lower plenum, and core*

In the nodalization diagram and based on symmetry, the plant is simplified to a one-equivalent loop. The nodalizations of the primary and secondary loops are shown in Fig. 4a, whereas those of the core and lower plenum are shown in Fig. 4b. The nodalization scheme of the core (including the lower plenum) was segmented into four concentric radial rings and 24 axial levels. Axial levels 9–24 represent the active core region, and levels 1–7 correspond to the lower plenum. The support plate was located

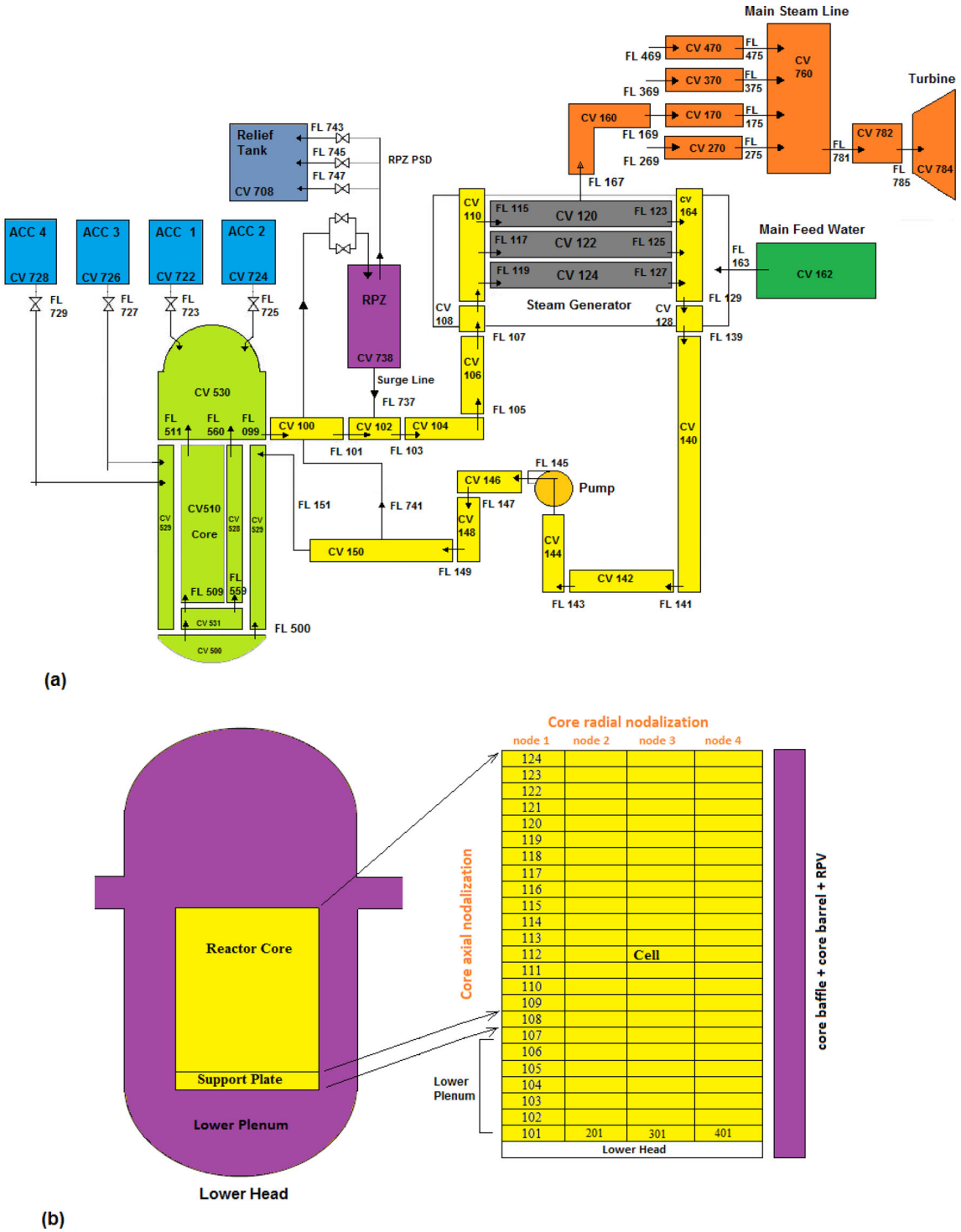

Fig. 4 (Color online) Nodalizations of primary loop, secondary loop, and core. **a** Primary and secondary loops; **b** core and lower plenum

at level 8. In addition, the lower plenum was segmented into four concentric radial rings.

2.3.3 Cavity and CC modeling

Figure 5 shows the cavity, CC, and in-containment refueling water storage tank (IRWST), which were modeled using the MELCOR code. In this study; the cavity, CC system, and IRWST were modeled as follows:

- The cavity was modeled using CV806 including the concrete inside, the materials of which are listed in Table 5;
- the CC system was modeled using CV807, including the CV806 volume; the sacrificial materials were layered in the CC volume;
- the IRWST is used to supply water around the CC and was modeled according to CV 808.

Table 6 lists the sacrificial materials used in the CC system. It is noteworthy that the composition of the sacrificial material was selected based on the optimal composition obtained from the Komlev project [12], in which the new sacrificial material was analyzed. In this study, 160 tons of SM in a CC system was assumed.

Table 5 Composition of concrete cavity materials used in BNPP [21]

Parameter	Rate
Average temperature (K)	1470
Fe (%)	16.2
H_20 evap (%)	3.1
SiO_2 (%)	47.4
CaO (%)	20
CO2 (%)	6.76
Al_2O_3 (%)	1.76
Fe_2O_3	2
MgO	1.1
Total density (kg/m^3)	2600

Table 6 Composition of sacrificial material for modeling CC system

Compositions	Mass fraction of material (%)	Mass (Kg)
Fe_2O_3	60	96,000
Al_2O_3	28	44,800
SiO_2	2	3200
SrO	5	8000
CaO	5	8000

3 SBO accident description as BDBA

An SBO as a BDBA is considered to be a severe accident that melts the core. The LOOP (whose probability is 26% of total possible BDBAs, c.f., [18]) and the loss of all diesel generators (due to earthquake, etc.) result in an SBO [30]. SBO (as a major severe accident) was fully analyzed in our previous study [18]. If operators cannot manage a plant, core melting will occur. It is noteworthy that SBO accidents without the feed and bleed strategy [18], core heat-up will begin to occur at 8900 s (using ECCS, second column Table 7). Subsequently, based on the current study, the core will melt at 28,300 s. Table 7 presents the main time-event sequences provided in the plant FSAR. In the

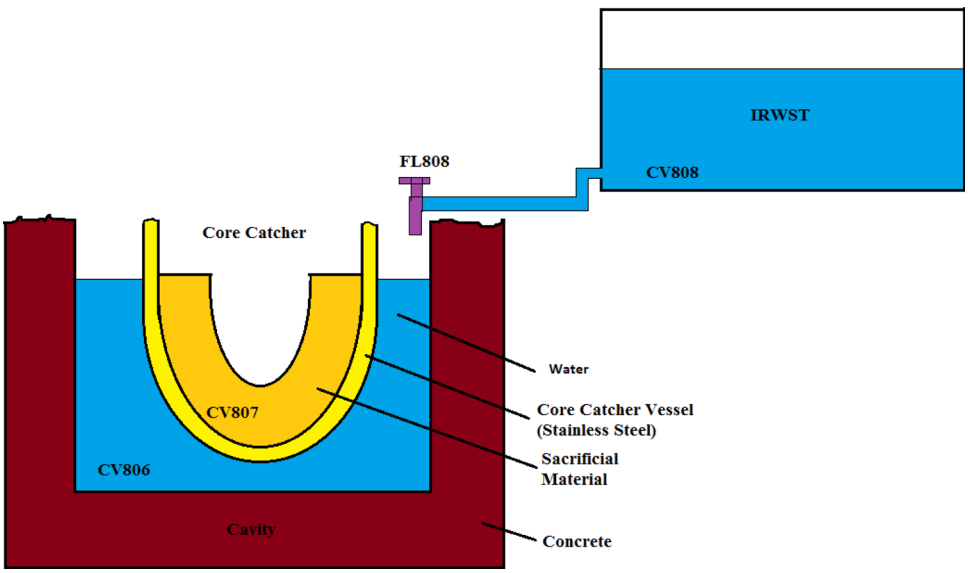

Fig. 5 (Color online) Schematic illustration of cavity, CC, and IRWSRT from MELCOR

Table 7 SBO accident sequences for different scenarios

Events and/or sequences	FSAR: without operator action [19]	FSAR: Feed and bleed in primary side [19]
Trip of all RCP sets	0.0	0.0
Trip of main and auxiliary feedwater systems of secondary side		
Trip of makeup-blowdown system of primary system		
BRU-K disconnection		
Disconnection of PRZ system power supply		
Closing of turbine generator stop valves	0.6	0.6
Scram signal generation	1.4	1.4
Onset of control rod motion	1.7	1.7
BRU-A opening	5.0	5.0
Closing of FSIV in secondary side, and secondary side depressurization	–	–
Connection of deaerator to 4th SG (SG-4)	–	–
SG drainage	2800	2800
Opening of control PRZ PSD valves to decrease pressure (in overpressure protection mode)	3880	3880
Opening of one PRZ PSD and valves on gas removal lines by operator	–	5000
Actuation of ACCs	–	7700
Actuation of KWU tanks	–	–
Onset of core heat-up	7000	8900
End of calculation	10,000	10,000

current study, we referred to the formal FSAR report (c.f., Table 7).

4 Benchmarking

4.1 Containment pressure validation based on LB-LOCA and ECCS

To validate the containment model, LB-LOCA was performed in cold-leg pipelines (diameter = 850 mm), and emergency core cooling systems (ECCS including KWUs and ACC emergency tanks) were used to manage the accident. Figure 6 shows a comparison of the pressure in the reactor containment for both the FSAR and current model; as shown, similar trends are presented.

The parameter settings used in the current simulation were as follows:

- The total containment air volume was V_{tot} = 71,040 m^3, based on Table 5.
- The containment contained heat sources, such as SGs and pipelines. Therefore, the effective temperature was within 55–70 °C at a pressure close to the atmospheric pressure (in the steady-state condition before the accident). In this case, the effective air density was 1.07 kg/m^3. The volume of each containment room is shown in Table 5. Therefore, the total mass of air in the containment can be computed easily, i.e., M_a = 76,012 kg.
- Consider a rupture of 850 mm in one loop. The four-loop was simulated as the average one-loop, where the water flow rate in the four-loop primary side was 84,800 m^3/h (in the steady state of the four-loop). A one-average-loop was assumed to simulate the four-loop. In this LB-LOCA case, $\frac{84,800}{4}$ = 21,200 m^3/h was the flow rate (source term) of hot water ejected from and injected into the containment. For instance, three hours after an accident, the amount of ejected water would be 63,600 m^3.
- The nominal reactor power was 3000 MWt in the steady-state condition before the accident onset.

Based on the initial conditions above, immediately after the LOCA, the resulting pressure and steam quality increased in the containment. The ECCS (including eight KWUs tanks and four ACC, c.f., Table 3) injects water into the primary system and core cooling after the accident. The fission fragment decay heat and the boiling crisis are two major heat sources in the containment. In addition, the ECCS is a heat sink that decreases the ejected water temperature. Based on the MELCOR simulations, the containment pressure was obtained, as shown in Fig. 6.

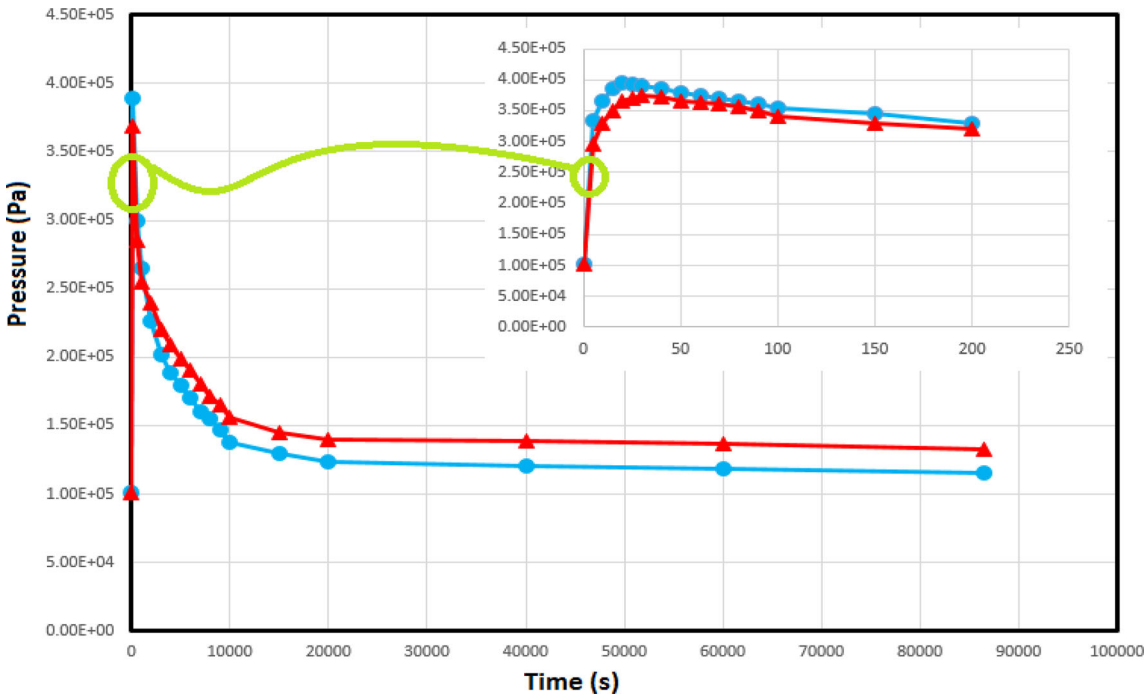

Fig. 6 (Color online) Containment pressure after LB-LOCA accident and including ECCS

4.2 Primary and secondary loop validation in steady state

The main parameters of the BNPP under steady-state conditions are summarized in Table 8, and they were verified in the current study. The relative errors obtained were less than the accepted criteria [31].

4.3 SBO validation

Although we have proposed innovative operational procedures for SBO management [18], the formal FSAR document was used for SBO benchmarking (c.f., Table 7). Using the SBO sequences provided in Table 7 and the MELCOR input, the primary pressure was obtained. Figure 7 shows the primary pressure following the SBO accident, with and without the ECCS.

5 Results and discussions

In the current section, we analyze the cavity and CC based on the obtained results. Specific explanations relevant to each subsection are provided. For the specific structures, please refer to Tables 5, 6, and 5. In addition, the following different conditions were considered:

(i) Dry cavity control volume in the CC without an ECCS, i.e., the dry cavity (state 1),
(ii) Wet cavity control volume in the CC without an ECCS, i.e., the wet cavity (state 2),

Table 8 Validation of steady-state main parameters with MELCOR input

No.	Parameters	VVER-1000 FSAR	MELCOR	|Error|%
1	Power (MWt)	3000	3000	N/A
2	Pressure in the primary circuit (MPa)	15.7	15.78	0.5
3	Inlet temperature in the core (°C)	291	291.1	0.03
4	Outlet temperature in the core (°C)	321	321.1	0.03
5	Pressure of steam generator secondary side, MPa	6.3	6.27	0.4
6	Outlet temperature of SG (°C)	279	278.7	0.1
7	Main feed-water flow rate (kg/s)	408.33	408.29	0.01
8	Main feed water temperature	220	220.1	0.05
9	Initial mass of UO_2 (kg)	79,840	79,840	N/A

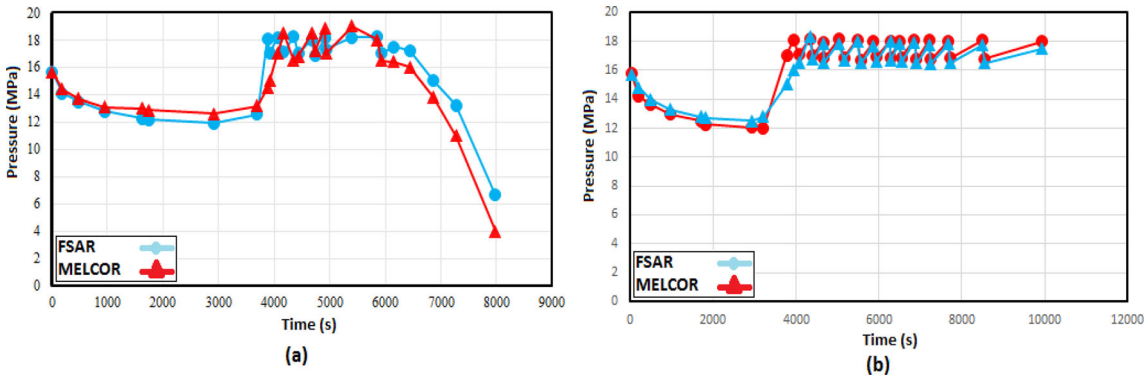

Fig.7 (Color online) Primary pressure with/without ECCS: **a** With ECCS; **b** without ECCS

(iii) Dry cavity control volume and dry CC control volume without an ECCS (state 3)
(iv) Wet cavity control volume and wet CC control volume without an ECCS (state 4).

The four states above were considered with the ECCS, and eight different states were analyzed in this study (c.f., Table 9). Figure 5 and Tables 5 and 6 provide more details regarding the CC and cavity.

5.1 Materials produced in lower plenum

Based on the current scenario, if the SBO accident cannot be efficiently managed, then the core will melt and the molten corium is transferred to the reactor's lower plenum; subsequently, it enters the cavity and CC. Table 10 lists the molten material provided in the lower plenum based on two cases, i.e., with/without the ECCS. Figure 8 shows the amount of molten corium transferred to the dry cavity, without a CC (state 1).

As shown in Fig. 8, the core melted at 16,430 s when the ECCS was not used, whereas the heart melted at 28,630 s when the ECCS was used.

The total amount of molten corium transferred into "state 1" was less in the case without the ECCS compared with that with the ECCS (c.f., Table 10). In addition, the molten UO_2 was much lower in the case without the ECCS.

Table 10 Amount of molten material provided in lower plenum and transferred into dry cavity, without CC (state 1)

Mass of material (Kg)	Without ECCS	With ECCS
Fuel	2445	14,426
Zircaloy	5598	2397
ZRO_2	1481	1030
Steel	31,545	15,836
Steel oxide	413.8	221.1
Control poison	77.68	26.04
Mass of H_2O consumed	3864	2392
Mass of H_2 produced	432.4	267.6
Hydrogen produced by SS	15.78	14.25
Hydrogen produced by Zircaloy	414.9	251.7
Hydrogen produced by B_4C	1.745	1.686
Mass of CO produced	1.437	2.245
Mass of CO_2 produced	2.785	1.516
Total corium mass at lower plenum	150,400	156,710

The total amount of hydrogen was a major concern, and it was greater in the case without the ECCS. The details of the suggested material are shown clearly for both cases.

Table 9 Suggested conditions (states) for cavity and CC in current study

Number states	Description of state	ECCS condition
State 1	Dry cavity, without CC	Without ECCS
State 2	Wet cavity, without CC	Without ECCS
State 3	Dry cavity + dry CC	Without ECCS
State 4	Wet cavity + CC with water inside	Without ECCS
State 5	Dry cavity, without CC	With ECCS
State 6	Wet cavity, without CC	With ECCS
State 7	Dry cavity + dry CC	With ECCS
State 8	Wet cavity + CC with water inside	With ECCS

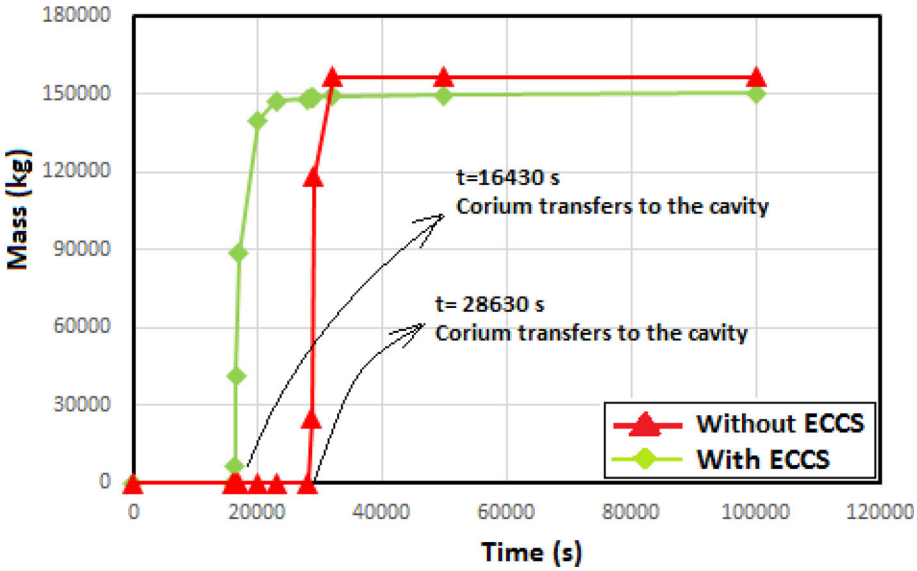

Fig. 8 (Color online) Comparison of amount of corium provided in lower plenum and transferred to dry cavity, without CC

5.2 Materials formed in cavity

The total mass formed in the cavity based on the time-dependent conditions is shown in Fig. 9a, and the amount of hydrogen produced is shown in Fig. 9b.

5.3 Ablation depth of cavity

The axial and radial ablation depths of the cavity concrete are directly related to the corium mass. Generally, the higher the corium mass and temperature, the more significant is the ablation of the concrete cavity, which causes a larger radial depth, as shown in Figure 10.

Figure 11 shows the ablation depth of the concrete in the radial and axial directions and for different states. As shown in Fig. 11a, the largest concrete ablation depth in the radial direction was obtained in the dry cavity and "without ECCS" case, whereas the smallest in the wet cavity and without ECCS case. The same behaviors were observed in the axial direction, as shown in Fig. 11b.

5.4 Containment pressure and temperature

Figure 12a shows the computation results for the pressure of the containment (for 4 d after the SBO accident), in which different states without the ECCS were considered. Figure 12b shows the containment pressure with the ECCS. As shown in Fig. 12a, the highest and lowest containment pressures occurred in states 2 and 4, respectively. In addition, as shown in Fig. 12b, the highest and lowest pressures in the containment occurred in states 1 and 4, respectively. When the ECCS system was activated, the molten temperature was lower than that of the without ECCS case; meanwhile, when the corium entered the water pool, less steam was produce. Therefore, the dry cavity yielded the highest pressure owing to the MCCI. The

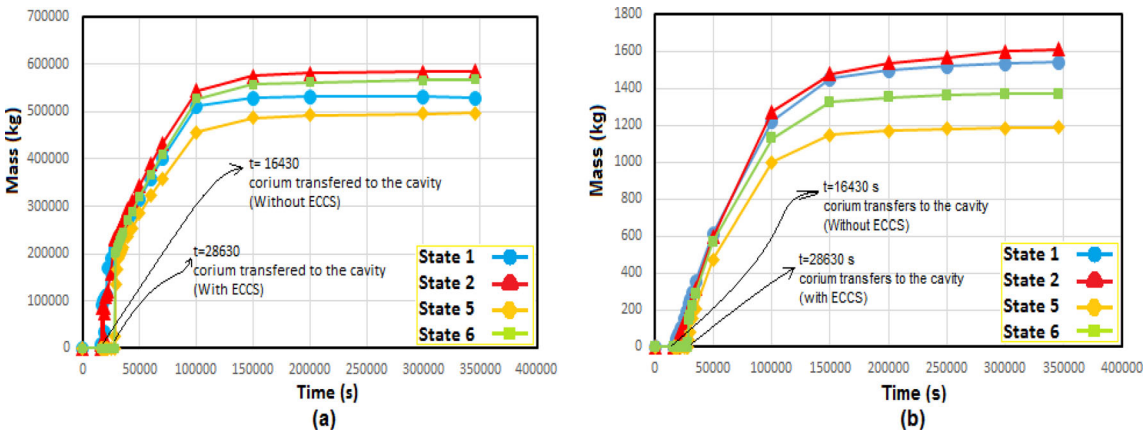

Fig. 9 (Color online) Total mass formed in cavity in different states for both with/without ECCS. **a** Mass formed in cavity (including corium + concrete); **b** amount of hydrogen

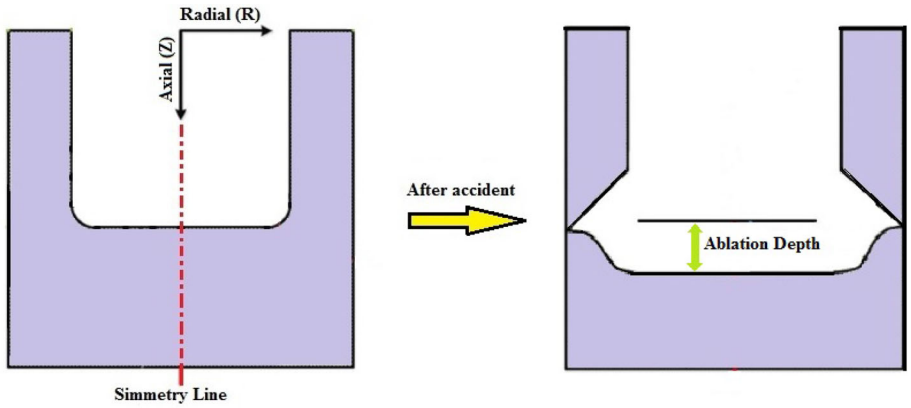

Fig. 10 (Color online) Cavity radius and height changes during accident

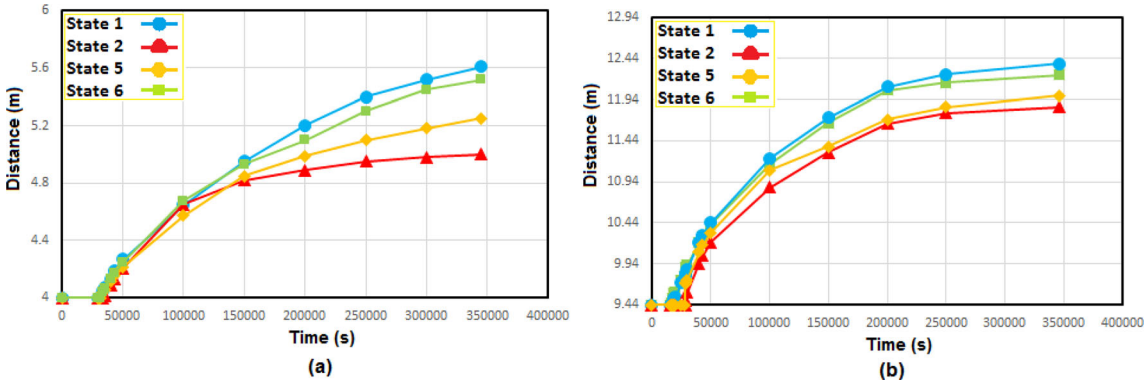

Fig. 11 (Color online) Comparison of radial and axial ablation depths of concrete cavity in dry and wet states, with/without ECCS. **a** Radial ablation; **b** axial ablation

current phenomena resulted in more voids owing to the corium being deposited into the water, and this may result in steam explosion.

The containment temperatures for cases without and with the ECCS are shown in Fig. 12c, d, respectively. It is clear that the highest containment temperature was in state 1, whereas the lowest was in state 4. If the ECCS is activated, then the highest and lowest temperatures will be recorded in states 6 and 8, respectively (c.f., Fig. 12d).

5.5 Gases in containment

In this section, the amounts of gases such as hydrogen, carbon, carbon dioxide, and nitrogen produced by the MCCI are explained.

The decrease in the hydrogen explosion probability of the containment is an important issue. Hence, we focused on the hydrogen production amount of the containment, which is illustrated in Fig. 13a, b for different states. The highest and lowest production amounts were recorded in states 2 and 4, respectively. Figure 13b shows that the highest and lowest hydrogen production amounts were recorded in states 5 and 8, respectively. Figure 13c, h show other gases that were produced in the containment.

Table 11 shows a summary of the results. The final results are indicated clearly. For instance, water around the CC resulted in a lower hydrogen production than the other states. Hence, we provided a (✔) mark for that case. A similar check-mark rule was applied for another case study and different states.

5.6 Theoretical Benchmarking of Best Result

Based on the MELCOR simulation, it was discovered that "Cavity + CC including water around" provided the best result. It was clear that the corium, together with the vessel water, descended into the CC. The current section provides a theoretical investigation of the best simulation results, from which we developed a theoretical model.

First, consider a severe accident in which the core has completely melted and hence descends to the bottom of the pressure vessel. This situation is illustrated in Fig. 14. Subsequently, the corium together with the vessel water descend into the "Cavity + CC including water around". The molten mixture of fuel (UO_2), fission products, clad (Zircaloy), control rod material (B_4C), and all core-supporting structures (steel) are known as the corium. In the case described, the corium melt fills the lower plenum and

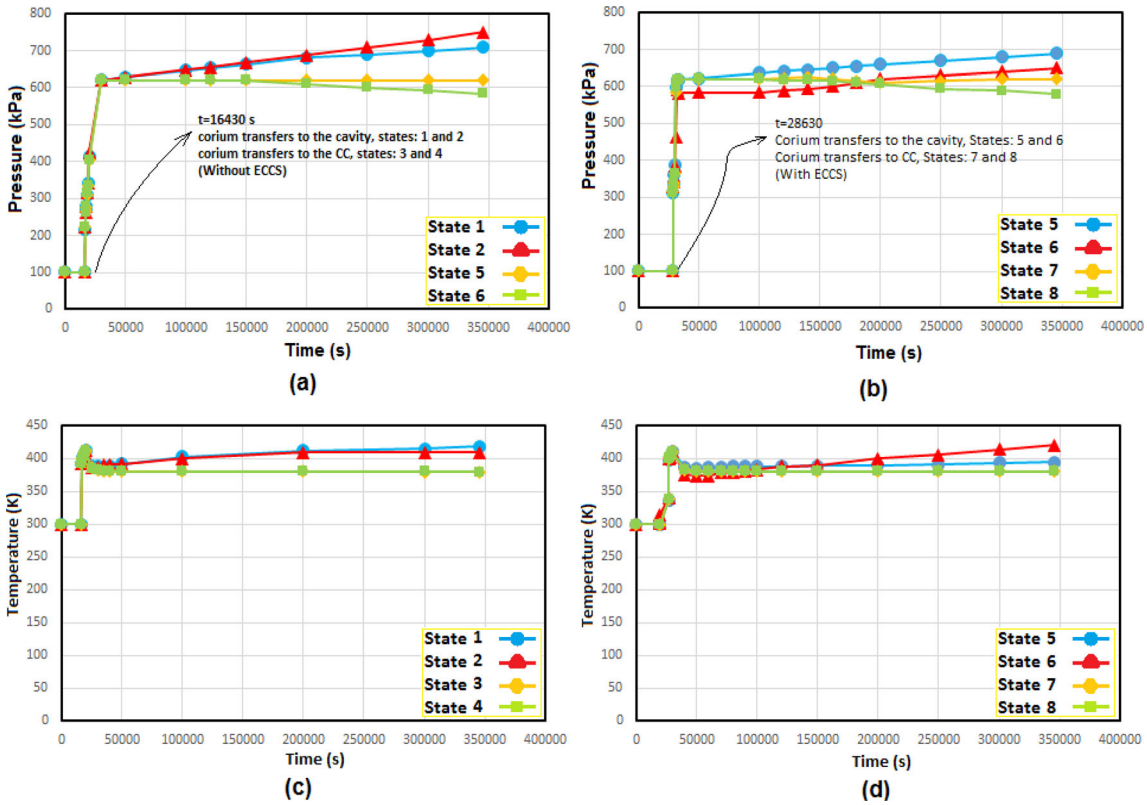

Fig. 12 (Color online) Containment pressure and temperature with/without ECCS for different states. **a** Pressure without ECCS; **b** pressure with ECCS; **c** temperature without ECCS; **d** temperature with ECCS

then moves to the CC system up to the hemispherical lower head. Water is present above the corium and outside the CC. The fuel decay heat is removed by boiling above the corium as well as by conduction through the CC wall (with boiling water outside the CC, which is the heat sink for the heat removal mechanism).

The corium temperature is denoted by T_c. Prior to the accident, the core thermal power was P_0 MWt. In this case, two-phase fluids occurred around the CC, and the temperature of the inside water (above the corium) is denoted as T_{wi}.

The water in the above-mentioned problem was in the film-boiling regime with radiation conflict. In this case, the film-boiling heat transfer correlations (in terms of W/m^2 C) can be determined based on Berenson [32], as follows:

$$h_{FB} = h_{conv} + 0.75h_{rad}, \tag{1}$$

where the convection and radiation coefficients are expressed as

$$h_{conv} = 0.425\frac{k_g}{\lambda_{conv}}\left[\frac{g(\rho_f - \rho_g)\rho_g\lambda_{conv}^3 h_{fg}}{k_g\mu_g T_{sat}}\right]^{0.25}, \tag{2}$$

$$h_{rad} = \sigma_{SB}\frac{(T_{wi}^4 - T_{sat}^4)}{(T_{wi} - T_{sat})}, \tag{3}$$

Here, $T_{wi} - T_{sat} = 0.01$ K is the difference between the corium two-phase water temperature above (at a constant pressure) and the saturated water. In this equation, T_{sat} and T_{wi} should be expressed in units of Kelvin.

$$\lambda_{conv} = 2\pi\sqrt{\frac{\sigma}{g(\rho_f - \rho_g)}}, \tag{4}$$

where σ is the surface tension.

Meanwhile, the energy balance for the corium melt is a combination of the decay heat as the source term and two removal terms, i.e., boiling in the water and conduction in the CC thickness. It can be expressed as shown in the following differential equation:

$$M_c C_c\frac{dT_c}{dt} = P_{decay} - P_{boiling} - P_{conduction}, \tag{5}$$

where c represents the corium. P_{decay} is the fission fragment decay heat power t seconds after the scram and is a positive source term expressed as

$$P_{decay} = 0.065P_0 t^{-0.2} \tag{6}$$

where P_0 is the power before scramming in terms of MWt,

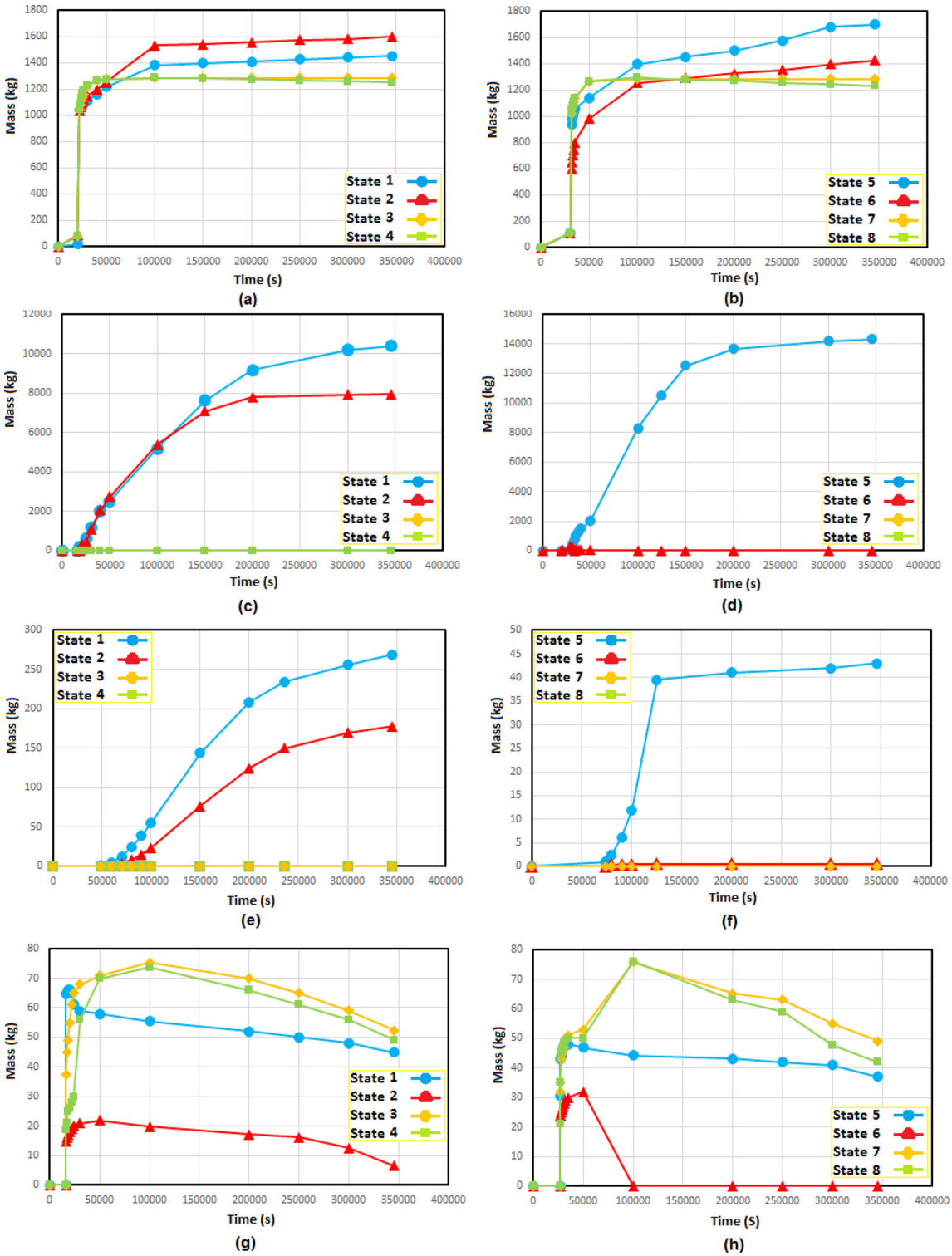

Fig. 13 (Color online) Gas production rates in containment with/without ECCS. **a** Hydrogen, without ECCS; **b** hydrogen, with ECCS; **c** CO, without ECCS; **d** CO, with ECCS; **e** CO_2, without ECCS; **f** CO_2, with ECCS; **g** N_2, without ECCS; (h) N_2, with ECCS

and t should be expressed in units of seconds. The conduction heat transfer between the corium and CC thickness (including the steel and concrete parts) is determined based on the following approximation:

$$P_{\text{conduction}} = k_{\text{V}}\left(\frac{T_{\text{c}} - T_{\text{Wo}}}{\Delta}\right) \times (\text{Hemispherical surface}), \tag{7}$$

Table 11 Summary of results for different states analyzed

State/parameter	ECCS condition	Dry cavity without CC	Wet cavity without CC	Dry cavity + CC without water around	Cavity + CC with water around
Containment Pressure	With ECCS Without ECCS				✔
Containment temperature	With ECCS Without ECCS				✔
Production of Hydrogen in containment	With ECCS Without ECCS				✔
Production of CO in containment	With ECCS Without ECCS				✔
Production of CO_2 in containment	With ECCS Without ECCS				✔
Production of N_2 in containment	With ECCS Without ECCS		✔		

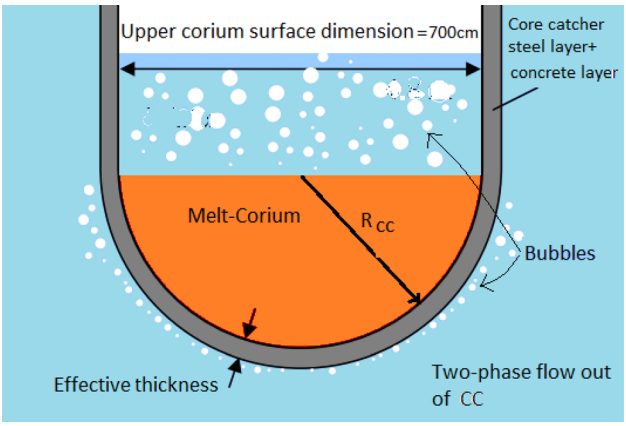

Fig. 14 (Color online) Illustration of corium entering from bottom of CC, resulting in two-phase fluid at the top and around the CC

where k_V represents the effective CC conduction coefficient (steel + concrete), T_{Wo} is the outside CC water temperature, and Δ is the effective CC thickness. The contact area is a hemispherical surface, $2\pi R_{cc}^2$, where R_{cc} is as shown in Fig. 14.

Finally, the boiling term inside the CC (above the corium) is expressed as

$$P_{\text{boiling}} = h_{FB}(T_c - T_{sat}) \times \left(\text{Upper surface above corium} = \pi R_{cc}^2\right), \quad (8)$$

The saturation temperature T_{sat}, upper disc-shaped area, and other related data are listed in Table 12.

The theory above was benchmarked with the best simulation result. Figure 15 shows a comparison of the results of the MELCOR calculations with those from theoretical investigation.

6 Conclusion

In the current study, a CC and its cavity were assessed for the VVER-1000/v528 containment. Specifically, after core melting following an SBO accident, various models were evaluated using the MELCOR1.8.6 code, where an ex-vessel CC was simulated for various subjects.

First, MELCOR benchmarking was considered for three different scenarios, i.e., LB-LOCA, SBO, and steady-state operations. The main objective of performing benchmarking was to be the core melting subsequence of the SBO for operations with and without an ECCS. After verifying the input, we defined eight states, which included different combinations of the cavity and CC (c.f., Table 9). By defining the eight states mentioned above and various boundaries of water, corium transfer (from the lower plenum) was investigated. The following parameters were investigated in different states:

- Containment pressure and temperature;
- production of different gases such as hydrogen, CO, CO_2, and other gases in containment; in addition, hydrogen production and axial–radial ablation in the CC were investigated.

"Wet cavity + Core Catcher with water inside; without/with ECCS" was denoted as states 4 and 8, respectively. It was discovered that state 8 yielded the best result; therefore, that the above-mentioned parameters yielded the best and/or worst results (c.f., Table 11).

Finally, a theoretical study was performed to benchmark the best result indicated by state 8. A decrease in the corium temperature was reflected in both the theoretical and MELCOR simulations.

Based on the results obtained, it was revealed that a CC system with an internal sacrificial material caused the

Table 12 Saturated water data at atmospheric pressure, and other useful data for theoretical investigations

Parameter	Value	Hint
ρ_f	960 kg/m^3	Hot fluid density at atmospheric pressure
ρ_g	0.6 kg/m^3	Void density at atmospheric pressure
$C_{p,f}$	4.2 kJ/kg °C	Thermal coefficient at constant pressure for fluid
$C_{p,g}$	2.1 kJ/kg °C	Thermal coefficient at constant pressure for void
μ_f	2.86×10^{-4} N s/m^2	Fluid viscosity at atmospheric pressure
μ_g	1.22×10^{-5} N s/m^2	Void viscosity at atmospheric pressure
h_f	419 kJ/kg	Atmospheric water enthalpy
h_g	2676 kJ/kg	Void enthalpy at atmospheric pressure
h_{fg}	1816 kJ/kg	Mixture of fluid–bubble enthalpy including 0.381 void fraction
k_g	0.02 kW/m °C	Void convection coefficient at atmospheric pressure
k_f	0.68 kW/m °C	Fluid convection coefficient at atmospheric pressure
σ_{SB}	5.67×10^{-8} W/m^2 K^4	Stefan–Boltzmann correlation coefficient
σ	0.06 N/m	Tensile coefficient
ε	0.4	Emissivity from Boltzmann relation
T_{sat}	100 °C = 373 K	Saturation temperature at atmospheric pressure
ρ_c	8000 kg/m^3	Corium density
ρ_{Vs}	7500 kg/m^3	Steel-layer density in CC
ρ_{Vc}	2400 kg/m^3	Concrete-layer density in CC
C_c	530 J/kg °C	Corium specific heat coefficient
K_{vs}	30 W/m °C	Steel-layer thermal conductivity coefficient
K_{vc}	1.5 W/m °C	Concrete-layer thermal conductivity coefficient
K_v	$\frac{(K_{vc}\times\Delta_c)+(K_{vs}\times\Delta_s)}{\Delta}$ W/m K	Effective thermal conductivity of CC thickness (steel + concrete)
Δ	1.5 m	Effective thickness of CC (steel + concrete)
Δ_s	0.1 m	Steel layer thickness of CC
Δ_c	1.4 m	Concrete layer thickness of CC
$2\pi R_{cc}$	76.93 m^2	Hemispherical surface of lower part of CC
πR_c^2	38.465 m^2	Surface area above corium
T_{wo}	$\approx$ 109 °C = 382 K	Outside CC water temperature; outside pressure exceeds atmospheric temperature
T_{sat}	$\approx$ 100 °C = 373 K	Saturated water inside CC and above corium at atmospheric pressure
$T_c(t = 0)$	$\approx$ 2000 °C	Corium temperature at initial time
$M_c(t = 0)$	150,400, kg©	Time-dependent corium mass in CC. It depends on the case study and reactor type
h_{FB}	c.f., Eq. (1) to (4) = 400 W/m^2 °C	Film boiling + radiation heat transfer coefficient
D	7 m	Internal width of CC
g	9.81 m/s^2	Gravitational acceleration
P_0	3000 MW = 3×10^6 W	Core power before scram

©It was assumed that at t = 0, all vessel corium was transferred into the CC

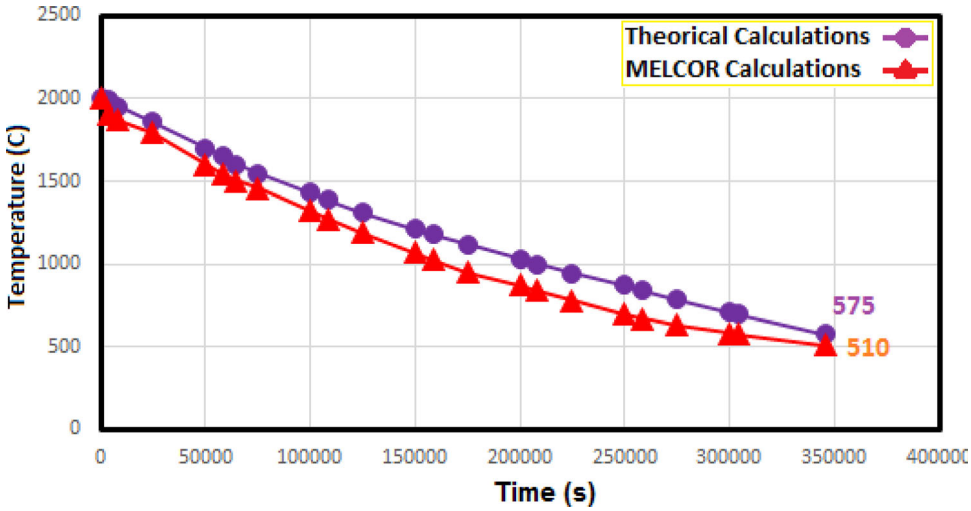

Fig. 15 (Color online) Comparison of corium temperature for both theoretical and MELCOR calculations (t = 0 is the time at which all corium and water descended into the CC)

pressure inside the containment to be reduced from 689 to 580 kPa and the temperature from 394 to 380 K. Furthermore, it was observed that the amount of gas produced, particularly hydrogen, decreased from 1698 to 1235, which was a reduction by 27.2%. Additionally, the results showed that the presence of supporting systems, including an ECCS system with a CC, prolonged the core melting time from 16,430 to 28,630 s in an SBO accident, whereas the thermal–hydraulic parameters and gases produced decreased significantly.

References

1. T.H. Vo, J.H. Song, An analysis of containment responses during a station blackout accident. J. Nucl. Sci. Technol. **54**, 1074–1084 (2017). https://doi.org/10.1080/00223131.2017.1344584
2. S.V. Svetlov, V.V. Bezlepkin, V.S. Granovsky. Core Catcher for Tianwan NPP with VVER-1000 reactor. Concept, Design and Justification. 11th International Conference on Nuclear Engineering Tokyo, Japan (2003). https://doi.org/10.1299/jsmeicone.2003.104
3. M. Weimin, Y. Yuan, B.R. Sehgal, In-vessel melt retention of pressurized water reactors: Historical review and future research needs. Engineering (2016). https://doi.org/10.1016/J.ENG.2016.01.019
4. O. Kumalanen, H. Tuomisto, T.G. Theofanous, In-vessel retention of corium of the Loviisa plant. Nucl. Eng. Design **169**, 109–130 (1997). https://doi.org/10.1016/S0029-5493(96)01280-0
5. T.G. Theofanous, C. Liu, S. Additon, In-vessel coolability and retention of a core melt. Nucl. Eng. Design **169**, 1–48 (1997). https://doi.org/10.1016/S0029-5493(97)00009-5
6. M.F. Rogov, I.V. Kukhtevich, V.B. Khabenskii et al., Analyzing the corium in the vessel of a VVER-640 reactor in a severe accident with a damaged core. Therm. Eng. **43**, 888–892 (1996)
7. G. Löwenhielm, A. Engqvist, R. Espefalt, Accident management strategy in Sweden and verification implementation. Nucl. Eng. Design **148**, 151–159 (1994). https://doi.org/10.1016/0029-5493(94)90106-6
8. Yu.A. Zvonarev, D.F. Tsurikov, V.L. Kobzar, Numerical analysis of core catcher efficiency for VVER-1200. Phys. At. Nucl. **74**, 1845–1853 (2011). https://doi.org/10.1134/S1063778811130084
9. V.B. Khabensky, V.S. Granovsky, S.V. Bechta et al., Severe accident management concept of the VVER-1000 and the justification of corium retention in a Crucible-Type core catcher. Nuclear Eng. Tecnol. **41**, 561–574 (2009). https://doi.org/10.5516/NET.2009.41.5.561
10. V. Astafyeva, V. Bezlepkin, V. Kukhtevich et al. Computational analysis of core catcher behavior during corium relocations from reactor vessel. Proceedings of the 18th International Conference on Nuclear Engineering, ICONE18–29860, Xi'an, China. 597–603 (2010). https://doi.org/10.1115/ICONE18-29860
11. A.A. Sulatsky, S.V. Bechta, V.S. Granovsky, Molten corium interaction with oxidic sacrificial material of vver core catcher. Proceedings of ICAPP '05, Korea, 5240 (2005).
12. A.A. Komlev, V.I. Almjashev, S.V. Bechta et al., New sacrificial material for ex-vessel core catcher. J. Nucl. Mater. **467**, 778–784 (2015). https://doi.org/10.1016/j.jnucmat.2015.10.035
13. M. Fischer, The severe accident mitigation concept and the design measures for core melt retention of the European Pressurized Reactor (EPR). Nucl. Eng. Design **230**, 169–180 (2004). https://doi.org/10.1016/j.nucengdes.2003.11.034
14. AEOI (Atomic Energy Organization of Iran). Final Safety Analysis Report (FSAR) for Bushehr VVER-1000 reactor, Chapter 6, Iran (2003).
15. M. Rahgoshay, M. Hashemi-Tilehnoee, Pressure distribution in the containment of VVER-1000 during the first seconds of large break LOCA. Prog. Nucl. Energy **88**, 211–217 (2016). https://doi.org/10.1016/j.pnucene.2016.01.010
16. F. Faghihi, S.M. Mirvakili, S. Safaei-Arshi et al., Neutronics and sub-channel thermal-hydraulics analysis of the Iranian VVER-1000 fuel bundle. Prog. Nucl. Energy **87**, 39–46 (2016). https://doi.org/10.1016/j.pnucene.2015.10.020
17. S. Bagheri, F. Faghihi, M.R. Nematolahi et al., Assessment of thermal hydraulics parameters of the VVER-1000 during transient conditions. Int. J. Hydrogen Energy **41**, 7103–7111 (2016). https://doi.org/10.1016/j.ijhydene.2016.02.066
18. M.M. Hosseini, F. Faghihi, A. Pirouzmand et al., Innovative passive management of the Station Black-Out accident for VVER1000/V446 NPP and development of its emergency operating procedures. Prog. Nucl. Energy **126**, 103–416 (2020). https://doi.org/10.1016/j.pnucene.2020.103416
19. AEOI (Atomic Energy Organization of Iran), Final Safety Analysis Report (FSAR) for BNPP, Chapter 15, Iran (2015).

20. R.O. Gauntt, J.E. Cash, R. K. Cole et al., MELCOR Computer Code Manuals, Vol. 1: Primer and Users' Guide Version 1.8.6. (2005).
21. R. Gharari, H. Kazeminejad, N. Mataji Kojouri et al., Study the effects of various parameters on hydrogen production in the WWER1000/V446. Prog. Nucl. Energy. 124, 103–370. (2020). https://doi.org/10.1016/j.pnucene.2020.103370
22. R. Gharari, H. Kazeminejad, N. Mataji Kojouri et al., Assessment of new severe accident mitigation systems on containment pressure of the WWER1000/V446. Ann. Nucl. Energy 148, 107691 (2020). https://doi.org/10.1016/j.anucene.2020.107691
23. P. Omidifard, A. Pirouzmand, K. Hadad et al., Analysis of loss of cooling and loss of coolant severe accident scenarios in VVER-1000/V446 spent fuel pool. Ann. Nucl. Energy **138**, 107205 (2020). https://doi.org/10.1016/j.anucene.2019.107205
24. O. Noorik, N. Jafari, M. Gei, Simulation of hydrogen distribution and effect of Engineering Safety Features (ESFs) on its mitigation in a WWER-1000 containment. Nucl. Sci. Tech. **30**, 97 (2019). https://doi.org/10.1007/s41365-019-0624-0
25. P.V. Petkov, D.V. Hristov, VVER-1000/V320 decay heat analysis involving TVS-M and TVSA fuel assemblies. Nucl. Eng. Design **238**, 3227–3239 (2008). https://doi.org/10.1016/j.nucengdes.2008.06.012
26. A.E. Stefanova, B.P. Groudev, P.P. Atanasova, Comparison of hydrogen generation for TVSM and TVSA fuel assemblies for water water energy reactor (VVER)-1000. Nucl. Eng. Design **239**, 180–186 (2009). https://doi.org/10.1016/j.nucengdes.2008.08.001
27. P. Groudev, A.E. Stefanova, R.V. Gencheva, Investigation of VVER 1000 core degradation during SBO accident scenario in case of pressurizer SV stuck in open position. *Technical Meeting on "Fuel Behaviour and Modelling Under Severe Transient and LOCA Conditions" Ibaraki, Japan*, (2011).
28. P. Groudev, A.E. Stefanova, R.V. Gencheva, Investigation of VVER 1000 fuel behavior in severe accident condition. *IAEA Technical Meeting "Modelling of Water-Cooled Fuel Including Design-Basis and Severe Accidents" 28 October – 1 November, Chengdu, China* (2013).
29. AEOI (Atomic Energy Organization of Iran). Atomenergoproekt, Preliminary safety analysis report of BNPP's VVER-1000 reactor, engineered safety features. Chapter 6, ed. Moscow (2017).
30. Atom Energo Proekt, *Probabilistic Safety Assessment of BNPP's VVER-1000 Reactor* (Ministry of Russian Federation of Atomic Energy, Moscow, 2014).
31. A. Petruzzi, F. Auria, Thermal-hydraulic system codes in nuclear reactor safety and qualification procedures. Sci Technol Nuclear Installations. **2008**, 460795 (2008). https://doi.org/10.1155/2008/4607995
32. N.E. Todreas, M.S. Kazimi, *Nuclear Systems I: Thermal Hydraulic Fundamentals* (Taylor & Francis, Milton Park, 1993).